Buckling Analysis of Thick Rectangular Flat SSSS Plates using Polynomial Displacement Functions

J. C. Ezeh, I. C. Onyechere, O. M. Ibearugbulem, U. C. Anya and L. Anyaogu

Abstract
The main focus of this work is on Buckling Analysis of Isotropic Thick Rectangular Plates using Polynomial Displacement Functions. The thick rectangular plate is subjected to uniaxial in-plane compressive loading, Nx. Orthogonal Polynomial Displacement Functions (OPDF) and a polynomial shear deformation function f(z) were used in deriving the direct governing equations for an isotropic thick rectangular plate. A thick rectangular plate with all the edges simply supported (SSSS) was considered for the detailed numerical study. Satisfying the boundary conditions for the SSSS plate, the direct governing equation was solved to obtain a simple analytical equation used in generating the non-dimensional critical buckling load parameters of the plates at different values of span-depth ratio (a/t) and aspect ratios (b/a). Results from the present study were compared with the works of other researchers to verify the validity of the present results.

Keywords: displacement functions, in-plane-displacements, out of plane displacement, thick plates, shear rotation, buckling and rectangular.

1. Introduction

In Structural Engineering, rectangular plates find numerous applications. The plates are mostly subjected to transverse, compressive and sometimes dynamic loads acting in the middle plane of the plate. When a plate is subjected to forces applied at the boundary parallel to the mid-plane of the plate and distributed uniformly over the plate's thickness, the state of loading is called an in-plane compressive loading [11]. In-plane loading causes a plate to buckle or become elastically unstable. The commencement of instability is called buckling [8]. Critical buckling load is the magnitude of the in-plane compressive axial forces at which the plate becomes unstable. If the in-plane compressive load applied to the plate are further increased beyond their critical values, very large deflections and bending stresses will occur which will eventually lead to complete failure of the plate. The famous classical plate theory (CPT) which neglects the effects of transverse shear deformation provides good results for thin plates only and over-estimates the critical buckling loads of thick plates. Mindlin [4], developed a displacement based first order shear deformation theory (FSDT) which considers the effect of transverse shear deformation by assuming linear variation of the in-plane displacements across the plate's thickness. These theories however, does not satisfy the zero traction boundary conditions on top and bottom surfaces of the plate and thus requires shear correction factor to satisfy the constitutive relations for transverse shear stresses and strains [8]. These drawbacks of the (CPT) and (FSDT) gave rise to the development of higher order shear deformation theories (HSDT). HSDT seek to get the realistic variation of the transverse shear strains and stresses through the thickness of plate by assuming parabolic (higher order parabolas) shear strain variation across the thickness [5].

Gunjal et al. [2] used a refined trigonometric shear deformation function in the buckling analysis of thick isotropic square and rectangular plates. Sayyad and Ghugal [8] used exponential shear deformation function to carry out bi-directional bending and free vibration analysis of thick isotropic square and rectangular plates. Sayyad and Ghugal [9] applied exponential shear deformation function in the buckling analysis of thick isotropic square plates subjected to uniaxial and biaxial in-plane loads. Akavci [1] worked on Buckling and free vibration analysis of symmetric and antisymmetric laminated composite plates on an elastic foundation using trigonometric shear deformation function. Rajesh and Meera [7] applied trigonometric functions as displacement and shear deformation functions in their work on 'linear free-vibration analysis of rectangular mindlin plates using coupled displacement field method. Hashemi and Arsanjani [3], used trigonometric functions as displacement and shear deformation functions in their work on Exact Characteristic Equations for Some of Classical Boundary Conditions of Vibrating Moderately Thick Rectangular Plates. Serdoun and Hamza-Cherif [10] worked on Free Vibration Analysis of Isotropic Plates by Alternative Hierarchical Finite Element Method Based on Reddy's C1 HSDT. In the present work, a polynomial shear deformation function and polynomial displacement functions were used for buckling analysis of isotropic thick rectangular plates with all edges simply supported.

2 Mathematical Formulation of the Present Theory

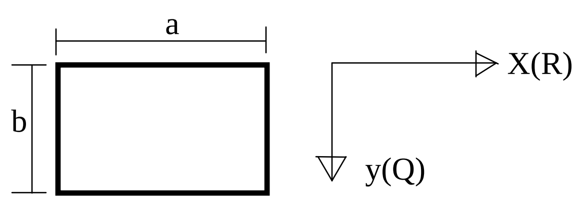

Figure 1: A Rectangular Plate.

J. C. Ezeh; jcezeh2016@gmail.com, I. C. Onyechere: onyecherechigozie@gmail.com, O. M. Ibearugbulem: ibeowums@gmail.com, U. C. Anya: collins.anya@futo.edu.ng and L. Anyaogu: engrdr.lewechi.anyaogu@gmail.com
All are lecturers at the Federal University of Technology, Owerri, Nigeria.

Consider an isotropic rectangular plate with length ‘a’ in x-direction, width ‘b’ in y-direction, and thickness ‘h’ in z-direction. The z-direction is assumed positive in downward direction. The plate occupies a region 0 ≤ x ≤ a, 0 ≤ y ≤ b, -t/2 ≤ z ≤ t/2 in Cartesian coordinate systems. The aspect ratio is P given as P = b/a. the non-dimensional coordinates (R = x/a and Q = y/b) occupy domain 0 ≤ R ≤ 1 and 0 ≤ Q ≤ 1. The aim of buckling analysis of plates is to determine the critical buckling loads.

Displacement Field: The displacement field include two in-plane displacements (u and v) and one out of plane displacement w. The displacement field (u, v and w) of the present theory are given by Onyechere (2018) as:

$$u = -z\frac{\partial w}{\partial x} + f(z).\emptyset_x \quad (1)$$

$$v = -z\frac{\partial w}{\partial y} + f(z).\emptyset_y \quad (2)$$

$$w(x,y) = w_x.w_y = (a_0 + a_1R + a_2R^2 + a_3R^3 + a_4R^4) * (b_0 + b_1Q + b_2Q^2 + b_3Q^3 + b_4Q^4) \quad (3a)$$

$$\emptyset_x = C_a.\frac{\partial w}{\partial x}, \quad \emptyset_y = C_b.\frac{\partial w}{\partial y}, \quad C_a \text{ and } C_b \text{ are constants} \quad (3b)$$

Where; f(z), Øx and Øy represent the shear deformation function, the shear rotations in x and y axes respectively.

Boundary Conditions: A close look at Equation (3a) shows that it is a product of two orthogonal beams; one in x(R)-axis and the other in the y(Q)-axis. The out-of-plane displacement, w for the two beams are given as Equations (4a) and (4b) respectively.

$$w_x = (a_0 + a_1R + a_2R^2 + a_3R^3 + a_4R^4) \quad (4a)$$

$$w_y = (b_0 + b_1Q + b_2Q^2 + b_3Q^3 + b_4Q^4) \quad (4b)$$

For the beam simply supported at both edges, the boundary conditions are as;

$$\text{(i)} At\ R = 0;\ w_x = 0, \frac{\partial^2 w_x}{\partial R^2} = 0 \ \text{(ii)} At\ R = 1;\ w_x = 0,\ \frac{\partial^2 w_x}{\partial R^2} = 0 \quad (5)$$

Substituting Equation (5) into Equation (3a), Equation (6) is obtained.

$$a_0 = 0, a_2 = 0, \quad a_1 = a_4, a_3 = -2a_4 \quad (6)$$

Substituting Equation (6) into Equation (3a), Equation (7a) is obtained.

$$w_x = a_4(R - 2R^3 + R^4) \quad (7a)$$

Similarly, repeating the same procedures for the beam in y (Q) - direction, Equation (7b) is obtained.

$$w_y = b_4(Q - 2Q^3 + Q^4)\ (7b).$$

Thus, for the rectangular plate simply supported at all edges, we obtain;

$$w = w_x.w_y = a_4(R - 2R^3 + R^4).b_4(Q - 2Q^3 + Q^4) \quad (8)$$

$$\mathrm{w} = J_1h = J_1(R - 2R^3 + R^4).(Q - 2Q^3 + Q^4) \quad (9)$$

$$Where;\ J_1 = a_4b_4, \quad h = (R - 2R^3 + R^4).(Q - 2Q^3 + Q^4) \quad (10)$$

h is the shape function for the SSSS thick plate, J_1 is the amplitude.

Substituting Equation (9) into (3b) gives;

$$\emptyset_x = J_2.\frac{\partial h}{\partial x} = \frac{J_2}{a}.\frac{\partial h}{\partial R} \quad (11a)$$

$$\emptyset_y = J_3.\frac{\partial h}{\partial y} = \frac{J_3}{b}.\frac{\partial h}{\partial Q} \quad (11b)$$

Where; $J_2 = C_a.J_1$, $J_3 =$ Cb.J1, J1, J2, J3 are coefficients of the displacement

Substituting equations (11a) and (11b) into equations (1) and (2) gives;

$$u = -z\frac{\partial w}{\partial x} + f(z).\emptyset_x = \frac{1}{a}.\left(-zJ_1\frac{\partial h}{\partial R} + f(z).J_2\frac{\partial h}{\partial R}\right) = \frac{1}{a}\frac{\partial h}{\partial R}.(-zJ_1 + f(z).J_2) \quad (12)$$

$$v = -z\frac{\partial w}{\partial y} + f(z).\emptyset_y = \frac{1}{b}\left(-zJ_1\frac{\partial h}{\partial Q} + f(z).J_3.\frac{\partial h}{\partial Q}\right) = \frac{1}{b}\frac{\partial h}{\partial Q}(-zJ_1 + f(z).J_3.) \quad (13)$$

Strain Displacement Relations.

Using strain-displacement relations of theory of elasticity, the strains used in the present theory are given as;

$$\varepsilon_x = \frac{\partial u}{\partial x} = \frac{1}{a}\frac{\partial \mathrm{u}}{\partial \mathrm{R}} = \frac{1}{a^2}\frac{\partial^2 h}{\partial R^2}.(-zJ_1 + f(z).J_2) \quad (14)$$

$$\varepsilon_y = \frac{\partial v}{\partial y} = \frac{1}{b}\frac{\partial \mathrm{v}}{\partial \mathrm{Q}} = \frac{1}{b^2}\frac{\partial^2 h}{\partial Q^2}(-zJ_1 + f(z).J_3.) \quad (15)$$

$$\gamma_{xy} = \frac{\partial u}{\partial y} + \frac{\partial v}{\partial x} = \frac{\partial u}{b\partial Q} + \frac{\partial v}{a\partial R} = \frac{1}{ab}\frac{\partial^2 h}{\partial R\partial Q}.(-zJ_1 + f(z).J_2) + \frac{1}{ab}\frac{\partial^2 h}{\partial R\partial Q}.(-zJ_1 + f(z).J_3.) \quad (16)$$

$$\gamma_{xz} = \frac{\partial u}{\partial z} + \frac{\partial w}{\partial x} = \frac{1}{a}\frac{\partial h}{\partial R}.\left(-J_1 + \frac{\partial}{\partial z}f(z).J_2\right) + \frac{1}{a}J_1\frac{\partial \mathrm{h}}{\partial \mathrm{R}} = \frac{\partial}{\partial z}f(z).J_2\ \frac{1}{a}\frac{\partial h}{\partial R} \quad (17)$$

$$\gamma_{yz} = \frac{\partial v}{\partial z} + \frac{\partial w}{\partial y} = \frac{1}{b}\frac{\partial h}{\partial Q}\left(-J_1 + \frac{\partial}{\partial z}f(z).J_3.\right) + \frac{1}{b}J_1\frac{\partial \mathrm{h}}{\partial \mathrm{Q}} = \frac{\partial}{\partial z}f(z).J_3\ \frac{1}{b}\frac{\partial h}{\partial Q} \quad (18)$$

Stress-Srain Relations: The stress-strain relations of the isotropic plate can be written as follows;

$$\sigma_x = \frac{E}{1-\mu^2}[\varepsilon_x + \mu\varepsilon_y] \quad (19)$$

$$\sigma_y = \frac{E}{1-\mu^2}[\mu\varepsilon_x + \varepsilon_y] \quad (20)$$

$$\tau_{xy} = \frac{E(1-\mu)}{2(1-\mu^2)}\gamma_{xy} \quad (21)$$

$$\tau_{xz} = \frac{E(1-\mu)}{2(1-\mu^2)}\gamma_{xz} \quad (22)$$

$$\tau_{yz} = \frac{E(1-\mu)}{2(1-\mu^2)}\gamma_{yz} \quad (23)$$

where E and µ are the Young’s modulus and the Poisson’s ratio of the material respectively.

Total Potential Energy: The total potential energy for the plate as derived in Onyechere, (2018) is given as;

ISSN 2229-5518

$$\begin{aligned}\Pi = U + V = \frac{1}{2}\int_x\int_y &[\sigma_x \varepsilon_x + \sigma_y \varepsilon_y + \tau_{xy}\gamma_{xy} + \tau_{xz}\gamma_{xz} \\ &+ \tau_{yz}\gamma_{yz}]dxdy \\ &- \frac{N_x}{2}\int_x\int_y \left(\frac{\partial w}{\partial x}\right)^2 \partial x \partial y \quad (24)\end{aligned}$$

Substituting equations 19 to 23 into Equation (24)gives;

$$\begin{aligned}\Pi = U + V = \frac{E}{2(1-\mu^2)}\int_x\int_y &\Big[{\varepsilon_x}^2 + 2\mu\varepsilon_x\varepsilon_y + {\varepsilon_2}^2 \\ &+ \frac{(1-\mu)}{2}{\gamma_{xy}}^2 + \frac{(1-\mu)}{2}{\gamma_{xz}}^2 \\ &+ \frac{(1-\mu)}{2}{\gamma_{yz}}^2\Big]dxdy \\ &- \frac{N_x}{2}\int_x\int_y \left(\frac{\partial w}{\partial x}\right)^2 \partial x \partial y \quad (25)\end{aligned}$$

Let; $Å = \int_{-t/2}^{t/2} z^2 dz = \frac{t^3}{12}, \quad Åg_1 = \int_{-t/2}^{t/2} z^2 dz$,

$$Åg_2 = \int_{-t/2}^{t/2} [zf(z)]dz \ , Åg_3 = \int_{-t/2}^{t/2} [(f(z))^2]dz$$

$$Å\frac{\propto^2}{a^2}g_4 = \int_{-t/2}^{t/2}\left[\frac{df(z)}{dz}\right]^2 dz\,,$$

$$D = \frac{ÅE}{1-\mu^2} = \frac{Et^3}{2(1-\mu^2)} \quad (26)$$

D is the flexural rigidity of the plate, and $\propto = {}^{a}/_{t}$ is the span-depth ratio.

Onyechere, (2018) in his work defined the dimensional shear deformation function as:

$$f(z) = z - \frac{7z^3}{5t^2} \quad (27a)$$

Thus, from Equation (27a), equations (27b) to (27e) are obtained:

$$\int_{-t/2}^{t/2}(z^2)dz = \left[\frac{z^3}{3}\right]_{-t/2}^{t/2} = \left(\frac{1}{3}\right)\left[\frac{t^3}{8} - -\frac{t^3}{8}\right] = 2\left(\frac{1}{3}\right).\left(\frac{t^3}{8}\right) = \frac{t^3}{12} \quad (27b)$$

$$\left(f(z)\right)^2 = z^2 - \frac{14z^4}{5t^2} + \frac{49z^6}{25t^4},$$

$$\int_{-t/2}^{t/2}\left(f(z)\right)^2 dz = \left[\frac{z^3}{3} - \frac{14z^5}{25t^2} + \frac{7z^7}{25h^4}\right]_{-t/2}^{t/2} = \frac{253t^3}{4800} \quad (27c)$$

$$zf(z) = z^2 - \frac{7z^4}{5t^2}\,,$$

$$\int_{-t/2}^{t/2} zf(z)dz = \frac{t^3}{12} - \frac{7t^3}{400} = \frac{79t^3}{1200} \quad (27d)$$

$$\left(\frac{df(z)}{dz}\right)^2 = 1 - \frac{42z^2}{5t^2} + \frac{441z^4}{25t^4}\,, \int_{-\frac{t}{2}}^{\frac{t}{2}}\left(\frac{df(z)}{dz}\right)^2 dz = \left[z - \frac{14z^3}{5t^2} + \frac{441z^5}{125t^4}\right]_{-\frac{t}{2}}^{\frac{t}{2}} = \frac{1041t}{2000} \quad (27e)$$

Substituting equations (14) to (18) and (26) into Equation (25) and multiplying each term by $\frac{a^4}{a^4}$ gave the total potential energy functional in terms on non-dimensional coordinates as:

$$\begin{aligned}\Pi = \frac{Dab}{2a^4}\int_0^1\int_0^1 &\Bigg[\left({J_1}^2g_1 - 2J_1J_2g_2 + {J_2}^2g_3\right)\left(\frac{d^2h}{dR^2}\right)^2 \\ &+ \left({J_1}^2g_1 - 2J_1J_3g_2 + {J_3}^2g_3\right)\frac{1}{P^4}\left(\frac{d^2h}{dQ^2}\right)^2 \\ &+ (2{J_1}^2g_1 - 2J_1J_2g_2 \\ &- 2J_1J_3g_2).\frac{1}{P^2}\left(\frac{d^2h}{dR^2}.\frac{d^2h}{dQ^2}\right) \\ &+ (1+\mu)J_2J_3g_3.\frac{1}{P^2}\left(\frac{d^2h}{dR^2}.\frac{d^2h}{dQ^2}\right) \\ &+ \left[\left(\frac{1-\mu}{2}\right)\left({J_2}^2g_3 + {J_3}^2g_3\right)\right].\frac{1}{P^2}\left(\frac{d^2h}{dR^2}.\frac{d^2h}{dQ^2}\right) \\ &+ \propto^2\left(\frac{1-\mu}{2}\right).\left({J_2}^2g_4\right)\left(\frac{dh}{dR}\right)^2 \\ &+ \frac{\propto^2}{P^2}\left(\frac{1-\mu}{2}\right)\left({J_3}^2g_4\right)\left(\frac{dh}{dQ}\right)^2\Bigg]dRdQ \\ &- \frac{ab{J_1}^2}{2}\int_0^1\int_0^1\left[\frac{N_x}{a^2}.\left(\frac{\partial h}{\partial R}\right)^2\right]\partial R\partial Q \quad (28)\end{aligned}$$

Where:

$$g_1 = \left(\frac{t^3}{12}\right)\Big/\left(\frac{t^3}{12}\right) = \frac{t^3}{12} * \frac{12}{t^3} = 1,$$

$$g_2 = \frac{79t^3}{1200}\Big/\left(\frac{t^3}{12}\right) = \frac{79t^3}{1200} * \frac{12}{t^3} = 0.79$$

$$g_3 = \frac{253t^3}{4800}\Big/\left(\frac{t^3}{12}\right) = \frac{253t^3}{4800} * \frac{12}{t^3} = 0.6325; \quad \frac{\propto^2}{a^2}g_4 = \frac{1041t}{2000}\Big/\left(\frac{t^3}{12}\right) = \frac{1041t}{2000} * \frac{12}{t^3} = \frac{6.246}{t^2}$$

$$g_4 = \frac{6.246}{t^2} * \frac{a^2}{\propto^2} = \frac{6.246}{t^2} * \frac{a^2}{1} * \frac{t^2}{a^2} = 6.246 \quad (29)$$

3 Direct Governing Equation.

Minimize the total energy functional with respect to J_1; J_2; J_3:

ISSN 2229-5518

$$\left(\frac{d\Pi}{dJ_1}=0, \frac{d\Pi}{dJ_2}=0, \quad \frac{d\Pi}{dJ_3}=0\right)$$

Minimizing equation 28 with respect to J1, J2 and J3 respectively gave:

$$\frac{D}{a^4}\left[\left(K_1g_1+\frac{K_3}{P^4}g_1+\frac{2K_2}{P^2}g_1\right)J_1+\left(-K_1g_2+\frac{K_2}{P^2}g_2\right)J_2 + \left(-\frac{K_3}{P^4}g_2-\frac{K_2}{P^2}g_2\right)J_3\right]=\frac{N_x}{a^2}K_4J_1 \quad (30a)$$

$$\frac{D}{a^4}\left[\left(-K_1g_2-\frac{K_2}{P^2}g_2\right)J_1 + \left(K_1g_3+\left(\frac{1-\mu}{2P^2}\right)K_2g_3 + \left(\frac{1-\mu}{2}\right)\propto^2 K_4g_4\right)J_2+\left(\left(\frac{1+\mu}{2P^2}\right)K_2g_3\right)J_3\right] = 0 \quad (30b)$$

$$\frac{D}{a^4}\left[\left(-\frac{K_3}{P^4}g_2-\frac{K_2}{P^2}g_2\right)J_1+\left(\left(\frac{1+\mu}{2P^2}\right)K_2g_3\right)J_2 + \left(\frac{K_3}{P^4}g_3+\left(\frac{1-\mu}{2P^2}\right)K_2g_3 + \left(\frac{1-\mu}{2P^2}\right)\propto^2 K_5g_4\right)J_3\right]=0 \quad (30c)$$

Where; $K_1=\int_0^1\int_0^1\left(\frac{\partial^2h}{\partial R^2}\right)^2\partial R\partial Q$,

$$K_2=\int_0^1\int_0^1\left(\frac{\partial^2h}{\partial R^2}.\frac{\partial^2h}{\partial Q^2}\right)\partial R\partial Q,$$

$$K_3=\int_0^1\int_0^1\left(\frac{\partial^2h}{\partial Q^2}\right)^2\partial R\partial Q,$$

$$K_4=\int_0^1\int_0^1\left(\frac{\partial h}{\partial R}\right)^2\partial R\partial Q, \qquad K_5=\int_0^1\int_0^1\left(\frac{\partial h}{\partial Q}\right)^2\partial R\partial Q$$

Re-writing Equations (30a), (30b) and (30c) in matrix form, yields Equation (31)

$$\begin{bmatrix}L_{11}&L_{12}&L_{13}\\L_{21}&L_{22}&L_{23}\\L_{31}&L_{32}&L_{33}\end{bmatrix}\begin{Bmatrix}J_1\\J_2\\J_3\end{Bmatrix}=\frac{a^4}{D}\begin{bmatrix}\frac{N_x}{a^2}K_4\\0\\0\end{bmatrix}\begin{Bmatrix}J_1\\J_2\\J_3\end{Bmatrix} \quad (31)$$

Equation (31) is the direct governing Equation for thick rectangular plates (using traditional third order shear deformation theory) of arbitrary boundary conditions.

Where; $L_{11}=g_1\left(K_1+\frac{2K_2}{P^2}+\frac{K_3}{P^4}\right), L_{12}=-g_2\left(K_1+\frac{K_2}{P^2}\right), L_{13} = -g_2\left(\frac{K_2}{P^2}+\frac{K_3}{P^4}\right), L_{21}=L_{12},$

$$L_{22}=K_1g_3+\left(\frac{1-\mu}{2P^2}\right)K_2g_3+\left(\frac{1-\mu}{2}\right)\propto^2 K_4g_4, L_{23} = \left(\frac{1+\mu}{2P^2}\right)K_2g_3,\ L_{31}=L_{13},\ L_{32}=L_{23},$$

$$L_{33}=\left(\frac{1-\mu}{2P^2}\right)K_2g_3+\frac{K_3}{P^4}g_3+\left(\frac{1-\mu}{2P^2}\right)\propto^2 K_5g_4 \quad (32)$$

The direct governing equation derived and presented in Equation (31) can be written as;

$$\begin{bmatrix}T_{11}&T_{12}&T_{13}\\T_{21}&T_{22}&T_{23}\\T_{31}&T_{32}&T_{33}\end{bmatrix}\begin{Bmatrix}J_1\\J_2\\J_3\end{Bmatrix}=\frac{a^2N_{xcr}}{D}\begin{bmatrix}1\\0\\0\end{bmatrix}\begin{Bmatrix}J_1\\J_2\\J_3\end{Bmatrix} \quad (33a)$$

Where; $T_{ij}=L_{ij}*{}^1/_{K_4}$

Equation (33a) is not coupled and thus, can be separated as:

$$\begin{bmatrix}T_{11}&T_{12}&T_{13}\end{bmatrix}\begin{Bmatrix}J_1\\J_2\\J_3\end{Bmatrix}=\frac{a^2N_{xcr}}{D}J_1 \quad (33b)$$

$$\begin{bmatrix}T_{22}&T_{23}\\T_{32}&T_{33}\end{bmatrix}\begin{Bmatrix}J_2\\J_3\end{Bmatrix}=-\begin{bmatrix}T_{21}\\T_{31}\end{bmatrix}J_1 \quad (33c)$$

Solving Equation (33c) using substitution method yields;

$$J_2=\left[\frac{-T_{23}.T_{31}+T_{33}.T_{21}}{T_{32}{}^2-T_{33}.T_{22}}\right]J_1, \qquad J_3 = \left[\frac{-T_{23}.T_{21}+T_{22}.T_{31}}{T_{32}{}^2-T_{33}.T_{22}}\right]J_1 \quad (34)$$

Substituting Equation (34) into equation (33b) gives;

$$T_{11}+T_{12}.\left[\frac{-T_{23}.T_{31}+T_{33}.T_{21}}{T_{32}{}^2-T_{33}.T_{22}}\right]+T_{13}.\left[\frac{-T_{23}.T_{21}+T_{22}.T_{31}}{T_{32}{}^2-T_{33}.T_{22}}\right] = \frac{a^2N_{xcr}}{D}=\theta_a \quad (35)$$

$Where; \theta_a = \frac{a^2N_{xcr}}{D}$ is a non $-$ dimensional critical buckling load parameter, (36)

4. Numerical Problems

The critical buckling load of the thick rectangular SSSS plate used in this work was sought. The stiffness coefficient obtained using the shape function, h = (R – 2R3 + R4)(Q – 2Q3 +Q4) are:

$$K_1=\int_0^1\int_0^1\left(\frac{\partial^2h}{\partial R^2}\right)^2\partial R\partial Q=0.23619; \quad K_2 = \int_0^1\int_0^1\left(\frac{\partial^2h}{\partial R^2}.\frac{\partial^2h}{\partial Q^2}\right)\partial R\partial Q=0.23592$$

$$K_3=\int_0^1\int_0^1\left(\frac{\partial^2h}{\partial Q^2}\right)^2\partial R\partial Q=0.23619; \quad K_4=\int_0^1\int_0^1\left(\frac{\partial h}{\partial R}\right)^2\partial R\partial Q = 0.0239; \ K_5=\int_0^1\int_0^1\left(\frac{\partial h}{\partial Q}\right)^2\partial R\partial Q = 0.0239 \quad (37)$$

Substituting these stiffness coefficients (Ki) and Equation 29 (gi) into equation 21 yields the T values (Tij).

Substituting these T values into Equation (35) yields the numerical critical buckling load parameters of the plate at various aspect ratios and span-depth ratios.

5 Results and Discussions

The critical buckling loads as determined herein for different aspect ratios and span-depth ratios are presented on Table 1.

Table 1: Results of the Present Study Compared with the Results of other Researchers for SSSS thick Plate.

		$P = {}^{b}/_{a}$						
		$N_{xcr} = \theta_a/12(1-\mu^2)$						
${}^{a}/_{t}$	Theory	1.0	1.5	2.0	2.5	3.0	3.5	4.0
5	Present Study (P.S)	2.9556	1.6255	1.2408	1.0783	0.9936	0.9455	0.9135
	Gunjal et.al (2015), (G)	2.9490	1.6620	1.2380	1.0760	0.9920	0.9430	0.9110
	Sayyad and Ghugal (2012), (S)	3.0260	1.6540	1.2590	1.0930	1.0070	0.9570	0.9250
	% Difference btw P.S & G	0.2238	2.1961	0.2262	0.2138	0.1613	0.2651	0.2744
	% Difference btw P.S & S	2.3265	1.7231	1.4456	1.3449	1.3307	1.2017	1.2432
10	Present Study (P.S)	3.4249	1.8155	1.3668	1.1790	1.0852	1.0279	0.9936
	Gunjal et.al (2015), (G)	3.4220	1.8120	1.3640	1.1780	1.0820	1.0260	0.9910
	Sayyad and Ghugal (2012), (S)	3.4540	1.8250	1.3730	1.1850	1.0890	1.0320	0.9970
	% Difference btw P.S & G	0.0847	0.1932	0.2053	0.0849	0.2957	0.1852	0.2624
	% Difference btw P.S & S	0.8425	0.5205	0.4516	0.5063	0.3489	0.3973	0.3410
20	Present Study (P.S)	3.5691	1.8704	1.4034	1.2088	1.1103	1.0508	1.0142
	Gunjal et.al (2015), (G)	3.5650	1.8670	1.4000	1.2060	1.1070	1.0490	1.0130
	Sayyad and Ghugal (2012), (S)	3.5820	1.8740	1.4050	1.2110	1.1110	1.0530	1.0160
	% Difference btw P.S & G	0.1150	0.1821	0.2429	0.2322	0.2981	0.1716	0.1185
	% Difference btw P.S & S	0.3601	0.1921	0.1139	0.1817	0.0630	0.2089	0.1772
50	Present Study (P.S)	3.6103	1.8864	1.4125	1.2179	1.1172	1.0577	1.0211
	Gunjal et.al (2015), (G)	3.6070	1.8830	1.4120	1.2160	1.1140	1.0570	1.0200
	Sayyad and Ghugal (2012), (S)	3.6210	1.8890	1.4150	1.2190	1.1180	1.0590	1.0220
	% Difference btw P.S & G	0.0915	0.1806	0.0354	0.1563	0.2873	0.0662	0.1078
	% Difference btw P.S & S	0.2955	0.1376	0.1767	0.0902	0.0716	0.1228	0.0881
100	Present Study (P.S)	3.6172	1.8887	1.4148	1.2179	1.1172	1.0600	1.0234
	Gunjal et.al (2015), (G)	3.6130	1.8850	1.4120	1.2160	1.1150	1.0570	1.0200
	Sayyad and Ghugal (2012), (S)	3.6250	1.8910	1.4160	1.2190	1.1190	1.0600	1.0230
	% Difference btw P.S & G	0.1162	0.1963	0.1983	0.1563	0.1973	0.2838	0.3333
	% Difference btw P.S & S	0.2152	0.1216	0.0847	0.0902	0.1609	0.0000	0.0391

From Table 1, it is observed that at the same span-depth ratio (a/t), the non-dimensional critical buckling load parameter decreases as the aspect ratio P = b/a increases having the highest value at P = 1 (square plate)..Also, at the same aspect ratio P = b/a, the non-dimensional critical buckling load parameter increases as the span-depth ratio increases. This indicates that the capacity of the plate to resist buckling decreases as the span-depth ratio, $(\propto = {}^{a}/_{t})$ increases. The percentage difference between the results of the present study and that of Gunjal et.al (2015), has a maximum value of 2.1961 at span – depth ratio of 5 and a minimum value of 0.0354 at span – depth ratio of 50. The percentage difference between the results of the present study and that of Sayyad and Ghugal (2012), has a maximum value of 2.3265 at span – depth ratio of 5, and a minimum value of 0.0000 at span – depth ratio of 100. This shows that as the span – depth ratio increases, the results of the present study becomes closer to that of Sayyad and Ghugal (2012). These differences being less than 5% are quite acceptable in statistics as being close. Thus, the present study provides a good solution for the buckling analysis of isotropic thick rectangular SSSS plate.

6. CONCLUSIONS.

Based on the results obtained from the present study, the following conclusions could be drawn:

(i) The general governing simultaneous equations developed and used in this work offer efficient and satisfactory results for buckling analysis of isotropic thick rectangular plates simply supported at its four edges.

(ii) The simple analytical equations developed and used in this work offer quick and satisfactory results for results for buckling analysis of isotropic thick rectangular plates simply supported at its four edges.

(iii) The critical buckling loads obtained in this work are very reliable as they agree with the works of other researchers. Thus, they can be used confidently by future researchers to design rectangular thick plates successfully.

7. REFERENCES.

[1] S. S. Akavci, "Buckling and free vibration analysis of symmetric and antisymmetric laminated composite plates on an elastic foundation," *Journal of Reinforced Plastics and Composites*, 26(18), pp 1907-1919, 2007.

[2] S. M. Gunjal, R. B. Hajare, A. S. Sayyad, and M. D. Ghodle, "Buckling Analysis of Thick Plates using Refined Trigonometric Shear Deformation Theory," *Journal of Materials and Engineering Structures*, Vol. 2, pp. 159–167, 2015

[3] S. H. Hashemi, and M. Arsanjani, "Exact characteristic equations for some of classical boundary conditions of vibrating moderately thick rectangular plates," *International Journal of Solid and Structures*, Vol. 42, pp. 819-853, 2004.

[4] R. D. Mindlin, "Influence of rotatory inertia and shear on flexural motions of isotropic elastic plates," *ASME Journal of Applied Mechanics*, Vol. 18, pp. 31-38, 1951.

[5] T. Nguyen-Thoi, T. Bui-Xuan, P. Phung-Van, H. Nguyen-Xuan, and P. Ngo-Thanh, "Static free-vibration and buckling analyses of stiffened plates using triangular elements," *Journal of Computers and Structures,* Vol.125, pp.100–111, 2013.

[6] I. C. Onyechere, "Stability and Vibration Analysis of Thick Plates using Orthogonal Polynomial Displacement Functions," PhD Thesis, Department of Civil Engineering, Federal University of Technology, Owerri (FUTO), Nigeria, unpublished.

[7] K. Rajesh, and S. K. Meera, "Linear free vibration analysis of rectangular Mindlin plates using coupled displacement field method," *Mathematical Models in Engineering*, Vol.1, Issue 1, pp. 41 – 47, 2016.

[8] A. S. Sayyad and Y. M. Ghugal, "Bending and free vibration analysis of thick isotropic plates by using exponential shear deformation theory" *Journal of Applied and Computational Mechanics*, Vol. 6, pp. 65–82, 2012.

[9] A. S. Sayyad and Y. M. Ghugal, Buckling analysis of thick isotropic plates by using exponential shear deformation theory. Journal of applied and computational mechanics, vol.6, pp. 185 – 196, 2012.

[10] S. M. N. Serdoun, and S. M. Hamza-Cherif, "Exact Characteristic Equations for Some of Classical Boundary Conditions of Vibrating Moderately Thick Rectangular Plates," *American Scientific Research Journal for Engineering, Technology, and Sciences (ASRJETS),* Volume 9, No 1, pp 1-19, 2014.

[11] S. Timoshenko, and J. M. Gere, "Theory of Elastic Stability," 2nd Edition, New York, McGraw-Hill Books Company, 1963.